Considering the suitability of symmetrical cell testing in developing electrodes for solid oxide fuel cells via a study of different lanthanum nickelate cathode materials

Harrison, C.M.; Klotz, D.; J.M. Sarruf, B.; Slater, P.R.; Steinberger-Wilckens, R.

DOI:
10.1016/j.ssi.2024.116551

Document Version
Publisher's PDF, also known as Version of record

Citation for published version (Harvard):
Harrison, CM, Klotz, D, J.M. Sarruf, B, Slater, PR & Steinberger-Wilckens, R 2024, 'Considering the suitability of symmetrical cell testing in developing electrodes for solid oxide fuel cells via a study of different lanthanum nickelate cathode materials', *Solid State Ionics*, vol. 411, 116551. https://doi.org/10.1016/j.ssi.2024.116551

Solid State Ionics 411 (2024) 116551

Contents lists available at ScienceDirect

Solid State Ionics

journal homepage: www.elsevier.com/locate/ssi

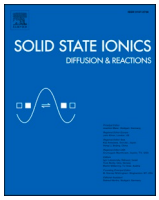

Considering the suitability of symmetrical cell testing in developing electrodes for solid oxide fuel cells via a study of different lanthanum nickelate cathode materials

C.M. Harrison [a,*], D. Klotz [c], B.J.M. Sarruf [a], P.R. Slater [b], R. Steinberger-Wilckens [a]

[a] Chemical Engineering Department, University of Birmingham, Edgbaston, Birmingham, B15 2TT, United Kingdom
[b] School of Chemistry, University of Birmingham, Edgbaston, Birmingham, B15 2TT, United Kingdom
[c] International Institute for Carbon-Neutral Energy Research (I²CNER), 744 Motooka, Nishi-ku, Fukuoka 819-0395, Japan (Ito Campus, Kyushu University)

ARTICLE INFO

Keywords:
SOC
SOFC
Lanthanum nickelates
Symmetrical
LSCF

ABSTRACT

Developing solid oxide fuel cells (SOFCs) with improved performance and lifetime continues to attract research attention from around the world. One important focus in this field is the synthesis of new air electrode materials that can replace the state-of-the-art lanthanum cobaltite-type phases. A host of materials with a wide range of properties has resulted. However, the means and metrics by which promising cathode materials are best characterised are not widely agreed upon within the literature and this can often complicate comparisons between studies. One common approach to conducting analysis of electrodes is to employ so-called 'symmetrical cell' tests which aim to isolate the performance of a specific electrode material under open-circuit conditions. However, despite the prevalence of symmetrical cell testing in the literature, there are some widely accepted limitations of the approach (e.g. limited to study at equilibrium conditions). In this work, a selection of air electrode materials with a wide range of properties were studied in both symmetrical and single cell testing set-ups. This case-study was conducted to identify the correlation between the two approaches and to understand how successful the symmetrical cell testing approach is in identifying favourable electrode materials. The results show that, whilst symmetrical-cell testing can be used to identify open circuit behaviours, the comparison between polarisation resistance at open circuit and performance under polarisation is not always perfectly correlated. Crucially, while the symmetrical cell test can provide some guidance in determining whether a new material may show promise, it highlights the need for more detailed studies to understand material performance under polarised conditions.

1. Introduction

1.1. Context

Solid oxide fuel cells (SOFCs) have received considerable laboratory and commercial interest over the course of many decades [1–3]. However, the deployment of the technology remains in an early commercial stage and further developments in performance will be required to accelerate market penetration. To this end, and with a view to reducing degradation rates, increasing lifetime and enhancing cell output, the development of SOFC components (e.g. air electrodes, i.e. cathodes) has proven an area of major research interest [2,4]. The underlying driver of this work has been to improve the cell performance.

1.2. Testing of SOFC cathode materials

There are a number of approaches to understanding the behaviour of a given material for SOFC applications. This includes study of fundamental properties (e.g. electronic conductivity via four point probe testing) or, alternatively, this can revolve around the use of in-situ testing methods (e.g. cell-level testing under polarisation). In the latter case, and in the example of SOFC cathodes, there are three possible approaches to testing electrodes; (1) two-electrode 'single cell' testing, (2) two-electrode 'symmetrical cell' testing or (3) three-electrode testing. Each of these approaches commonly draws on electrochemical impedance spectroscopy (EIS) techniques to help to identify the various resistive processes that ultimately determine performance losses. One approach is to employ reference electrodes (i.e. three-electrode testing)

* Corresponding author.
E-mail address: CMH725@alumni.bham.ac.uk (C.M. Harrison).

https://doi.org/10.1016/j.ssi.2024.116551
Received 5 February 2024; Received in revised form 21 March 2024; Accepted 9 April 2024
Available online 22 April 2024

to isolate the behaviour of a single electrode but, in SOFC testing, the placement of this electrode is non-trivial and the approach has not become a standard method [5–11]. The symmetrical cell testing approach has commonly been recommended as an alternative [10,11]. However, the limitation of the approach is that it restricts testing to equilibrium conditions (i.e. Open Circuit Voltage condition). Whilst this limitation is commonly acknowledged in the literature there is, to the best of our knowledge, no documented assessment of how fundamental such a constraint is.

In many publications, symmetrical cell testing is the only electrode-level test applied to compare the performance of electrode materials and microstructures. Single cell testing is often avoided. Results from symmetrical cell tests (i.e. R_{pol} values) are often referenced and compared in review literature. However, since symmetrical cell measurements are restricted to equilibrium conditions, it is reasonable to question how successful these tests are at identifying the electrode materials which are most adept at providing high current output. An alternative, and potentially more appropriate method, may be to consider current output at some defined voltages (e.g. 0.7 V) as in [2]. Although such measurements are influenced by other cell components and designs (e.g. anode design and electrolyte thickness), it is notable that deconvolution techniques (e.g. the Distribution of Relaxation Times modelling approach) have been the subject to much research and, with the correct experimental approach, this issue can be overcome. With such techniques becoming more widely employed it is appropriate to scrutinise the role of symmetrical cell testing.

In this paper, the value of symmetrical cell testing in determining the performance of electrodes is assessed. This is achieved via a study of different cathode materials ($La_2NiO_{4+\delta}$, $La_3Ni_2O_{7-\delta}$, $La_4Ni_3O_{10-\delta}$, $LaNi_{0.6}Fe_{0.4}O_{3-\delta}$, $La_{0.6}Sr_{0.4}Co_{0.2}Fe_{0.8}O_{3-\delta}$). These materials have also been assessed by other authors, both in terms of their fundamental properties (e.g. [12–21]) and in their performance when employed as SOFC electrodes (e.g. [18,21–29]). They are selected for the current analysis due to their differing and, in a sense, complimentary properties (i.e. materials ranging from those with excellent electronic conduction properties to those with excellent oxygen transport properties as is shown in [16,21]). Results are also reported for composite electrodes using $La_2NiO_{4+\delta}$ and $LaNi_{0.6}Fe_{0.4}O_{3-\delta}$ when employed with $Gd_{0.1}Ce_{0.9}O_{2-\delta}$ (GDC10) or $La_{0.45}Ce_{0.55}O_{2-\delta}$ (LDC45). Importantly, the consideration of different materials enables the testing methodologies to be more robustly assessed than would be the case if a relatively small sample of materials was considered. Comparisons between common metrics from symmetrical and single cell testing are drawn to establish how easily the results of these testing approaches can be related. In the first instance, the polarisation resistance results of single cell testing at Open Circuit Voltage (OCV) are compared with those from symmetrical cell testing. This is to first confirm the expected correlation of the two equilibrium-condition measurements. Secondly, impedance measurements conducted at OCV are compared against the findings from current measurements under polarisation. This is to determine whether a clear correlation can be found between the materials that perform well at OCV and those that provide the best current output under polarisation (e.g. the current density recorded at 0.7 V). The aforementioned selection of various cathode compositions was chosen to study if such relationships were consistent across electrodes with different behaviours. The comparison results in some interesting conclusions and the results have significant implications towards SOFC testing approaches.

2. Methodology

2.1. Materials synthesis

In this study, several lanthanum nickelate cathode materials ($La_2NiO_{4+\delta}$, $La_3Ni_2O_{7-\delta}$, $La_4Ni_3O_{10-\delta}$, $LaNi_{0.6}Fe_{0.4}O_{3-\delta}$) were synthesised via the Pechini process [30]. This approach has been widely employed in the literature (e.g. [29,31,32]) and is further detailed in the Supplementary Materials. The phase purity of the resulting powders was assessed via X-Ray Diffraction (XRD) analysis, using a D2 Diffractometer (Co K_α X-rays). Commercial $La_{0.6}Sr_{0.4}Co_{0.2}Fe_{0.8}O_{3-\delta}$ (Praxair) and $Gd_{0.1}Ce_{0.9}O_{2-\delta}$ (*Fuel Cell Materials*) were also utilised to represent a state-of-the-art composition for benchmarking purposes. Additionally, $La_{0.45}Ce_{0.55}O_{2-\delta}$ was synthesised via the Pechini process.

2.2. Electrode fabrication

After synthesis, each material was separately combined with an ink vehicle (Fuel Cell Materials) in a 2:1 volume ratio and homogenised using a triple roll-mill. For composite electrodes the cathode materials were mixed in a 1:1 volume ratio prior to the addition of the ink vehicle. The resulting cathode inks were applied to 25 cm^2 commercial cell substrates (SOFCMan) via brush painting, producing 16 cm^2 electrodes. To control the area and thickness of the electrodes, a 5 mm masking tape was applied to the substrates and an equal mass of ink was applied in each instance using a mass scale. The substrates employed for both symmetrical and single cell testing are described in Table 1. The wet electrode layers were dried at 100 °C and then sintered at high temperature (1000 °C or 1150 °C). In the case of single cell testing, additional samples were prepared using a sintering temperature of 1050 or 1100 °C. The described process followed an identical approach employed in our prior publication [33]. As in that study, commercial substrates were employed here to minimise the potential effects of inhomogeneities in cell components and to thus help to ensure that differences in results were caused only by differences in the cathode layers themselves.

2.3. Electrode testing

To provide a comparison between the single and symmetrical cell testing approaches a series of electrochemical experiments was performed, employing the two different testing configurations. A simplified schematic of these configurations is shown in Fig. 1 and described in further detail below. A full list of the tests conducted for this work is provided in Table S1 in the Supplementary Materials.

2.3.1. Symmetrical cell testing

Symmetrical cell testing was conducted in a horizontal Carbolite furnace. For each test, symmetrical cells were placed in a four-point probe testing set-up with current collection provided by a combination of gold paste (Fuel Cell Materials) and gold mesh (Fiaxell) as shown in Fig. 1a. These current collector materials were placed in contact with the two electrodes. Electrochemical Impedance Spectroscopy (EIS) measurements were conducted in air at temperatures between 600 and 800 °C in 50 °C intervals. These tests were conducted with a Solatron 1470E Potentiostat and a 1455 Frequency Response Analyser (FRA). For the measurements, a voltage perturbation of 10 mV was employed, using frequencies from 1 MHz to 0.05 Hz.

2.3.2. Single cell testing

Single cell testing (Fig. 1b) was performed using a commercial SOFC testing rig (Chino). Cells were assembled in an alumina housing with a

Table 1
– Substrates employed for cell testing in this study, as provided by SOFCMan. (*) For the $La_{0.45}Ce_{0.55}O_{2-\delta}$-based cathode composites, a $La_{0.45}Ce_{0.55}O_{2-\delta}$ interlayer was employed instead of GDC10 (YSZ coupons were procured without an interlayer and the LDC45 was applied via spin coating and sintered at 1200 °C).

Cell Type	Design
Symmetrical	<Cathode> | GDC10 (5 μm)*| YSZ (200 μm) | GDC10 (5 μm)* | <Cathode>
Single Cell	NiO-YSZ (400 μm) | YSZ (10–15 μm) | GDC10 (2–3 μm)* | <Cathode>

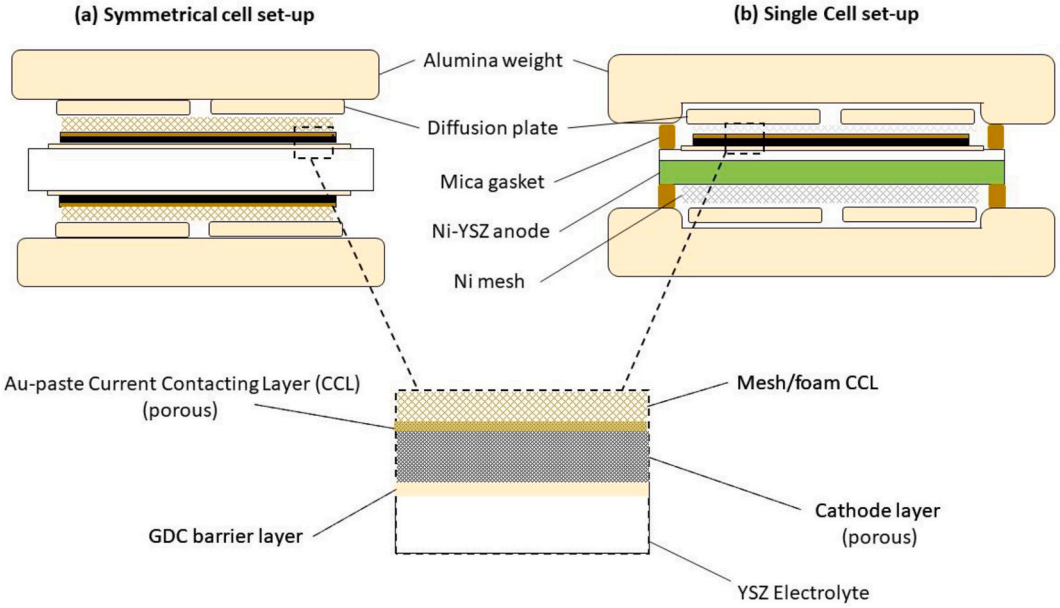

Fig. 1. Simplified schematic showing cell testing set-ups employed in this work; (a) symmetrical cell testing configuration and (b) single cell testing configuration.

four-point probe connection, allowing for separate voltage and current connections. Sealing on both sides of the cell was achieved using mica-frame gaskets. For the anode-side current collection, a nickel mesh (Chino) was placed in direct contact with the electrode. On the cathode side of the cell, the current collection was achieved using a commercial gold paste (Fuel Cell Materials) and silver mesh (Chino). The cell housing was placed in a Carbolite furnace and heated to 800 °C. The NiO anode was then reduced in a hydrogen/nitrogen mixture for 24 h. Both EIS and polarisation curves were acquired at temperatures from 800 °C down to 700 °C. For these tests, the anode and cathode were placed in humidified H_2 (500ml/min) and air (500 ml/min) atmospheres, respectively. To maintain a consistent level of humidification, a temperature-controlled bubbler was employed on the hydrogen line. The water tank was maintained at a consistent 35 °C. Measurements recorded with commercial cells (Supplementary Fig. S7) confirmed this approach to provide consistent results. In the case of EIS testing, a perturbation voltage of 50 mV was employed at frequencies from 1 MHz to 0.05 Hz. For polarisation curves, a potential-step approach was employed (as suggested in [11]), holding the voltage at 30 s at each point (10 mV voltage steps from OCV to 0.6 V). Voltages below 0.6 V were avoided given the impracticalities of operating under such conditions (e.g. cell damage and/or low efficiency). Preliminary testing of commercial cells found the described approach to provide consistent, repeatable results (see Supplementary Materials).

2.4. Data analysis

The EIS results were normalised by the apparent electrode area (S) and the R_{pol} results were obtained by the difference in the high (Z'_{HF}) and low (Z'_{LF}) frequency intercepts. In the case of the symmetrical cell testing approach, this was further divided by two to account for the number of electrodes, such that:

$$R_{pol} = \left(\frac{Z'_{LF} - Z'_{HF}}{2}\right) S \quad (1)$$

To test the stability of the impedance measurements, the Kramers-Kronig test was conducted via the Lin-KK software [34].

3. Results

3.1. Materials synthesis

XRD phase analysis of the lanthanum nickelate materials synthesised for this study is shown in Fig. 2. For comparison, the raw data are compared against literature data, as obtained from the ICSD database. As can be noted, single phase materials were achieved, with no observable impurity phases.

3.2. Symmetrical cell tests

Data from the symmetrical cell tests recorded at an operating temperature of 800 °C are shown in Nyquist plots in Fig. 3a and b. Results are shown for single phase electrodes sintered at 1000 °C and 1150 °C. Data for the LNO214 and LSCF6428 test points were reported in previous work [21]. The complete set of symmetrical cell data are provided in the Supplementary Materials (Fig. S1 to Fig. S3). The impedance measurements show very low Kramers-Kronig residuals with minimal noise, indicating very good quality data (Fig. S4 to Fig. S6). The R_{pol} results are summarised in the Arrhenius plots shown in Fig. 3c and d. Generally speaking, the lanthanum nickelate materials are seen to offer larger impedance values than the commercial LSCF6428 phase sintered at 1000 °C, although higher sintering temperatures improve the electrode performance of the nickelates. These observations are consistent with observations in our prior work [21,33]. Broadly, the performance of the single-phase lanthanum nickelate electrodes decreases (i.e. impedance values increase) with increasing n-value (R_{pol} values are shown to increase as follows; $La_2NiO_{4+\delta} < La_3Ni_2O_{7-\delta} < La_4Ni_3O_{10-\delta} \sim LaNi_{0.6}Fe_{0.4}O_{3-\delta}$). It can generally be noted that the polarisation resistance of the lanthanum nickelate materials decreases for those phases with inferior oxygen transport behaviour. Results from composite electrode tests can be viewed in the Supplementary Fig. S3 and are summarised in Table S2; the use of secondary oxide ion conducting phases is shown to improve the performance of the nickelate electrodes.

In the context of this work, it is not the main intention to remark on the absolute performance of the electrode materials in specific detail. It is, however, acknowledged that the reported polarisation results should not be regarded to be providing best-in-class electrode performance. Indeed, lower R_{pol} values have been achieved by other authors who have employed and optimised these same electrode materials (e.g.

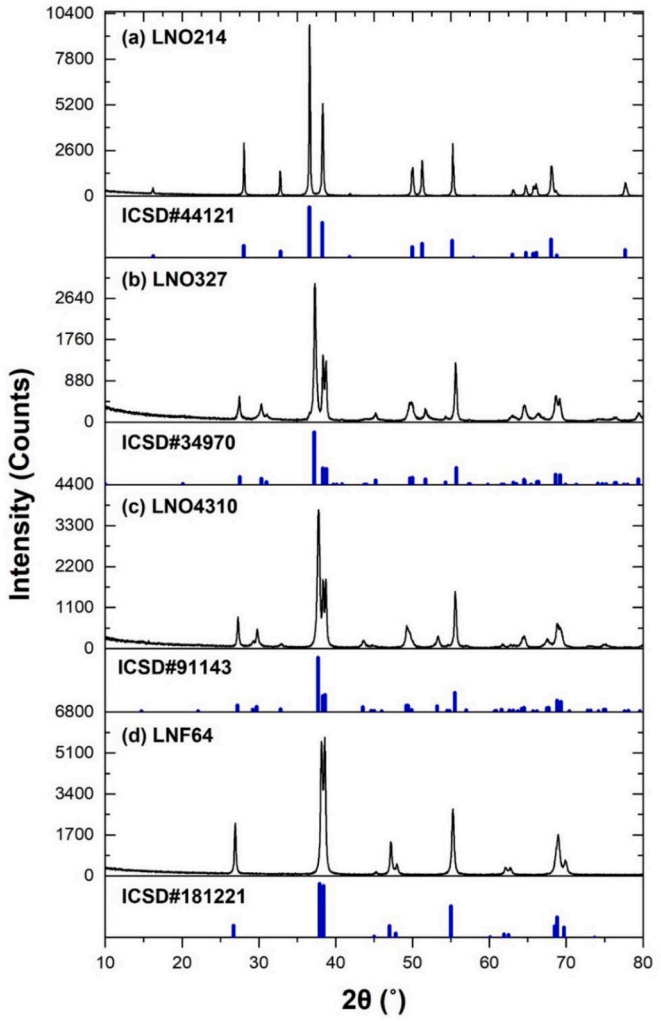

Fig. 2. XRD patterns of synthesised phases (top to bottom), (a) $La_2NiO_{4+\delta}$, (b) $La_3Ni_2O_{7-\delta}$, (c) $La_4Ni_3O_{10-\delta}$, (d) $LaNi_{0.6}Fe_{0.4}O_{3-\delta}$ denoted LNO214, LNO327, LNO4310, LNF64, respectively. A version of this figure has been published in a PhD thesis [35].

[22–24,27,28,36]). However, it is additionally noted that similar performance for these materials has also been reported in literature [18,22,28,37,38]. There are a number of possible causes for the observed range in R_{pol} values seen between studies (e.g. microstructure and particle size, contacting arrangement). The ability and extent of a single material to demonstrate a range of polarisation resistances was explored for LNF64 in [21] and for LNO214 in [33]. Given these observations, the results reported in the present work are deemed to be within an acceptable range for the intended purpose of the current work. Whilst it is noted that optimisation can achieve more favourable results, the focus of the present work is to consider how results from symmetrical cell testing compare with those of the single cell testing approach (see Section 3.3).

3.3. Single cell tests

Single cell testing results for studied electrodes are summarised in Fig. 4 at an operating temperature of 800 °C. Both polarisation data and EIS measurements recorded at open circuit voltage are shown. The complete set of data are provided in the Supplementary Material. Additionally, the Kramers-Kronig residuals for the impedance measurements are shown in Supplementary Fig. S14 to Fig. S16. In comparison with the symmetrical cell testing, the residuals are significantly larger, which is indicative of the difficulty of taking measurements in the single cells with the low impedance values of 25 cm^2 cells. However, the residuals show no systematic distribution which lets us conclude that they do not indicate any instability or even drift of the cells during measurement. For the sake of the analysis in this paper, we do not believe these residuals to represent a major point of concern.

It is notable from the results, there is a characteristic polarisation curve profile shape for each material; some, but not all, SOFC polarisation curves are found to be non-linear (other examples of this may be found in the wider literature (e.g. [39–41])). In the case of $La_2NiO_{4+\delta}$, a linear polarisation performance was observable, whereas, in the case of $LaNi_{0.6}Fe_{0.4}O_{3-\delta}$, a more curved profile was evident (showing greater losses in the activation region of the curve). As is shown in the Supplementary Material (Figs. S8 to S11), the 'shape' of these profiles was generally found to be consistent for each material across the different sintering temperatures. This indicates some phase-specific effects for each material, rather than an issue related to specific samples or the test set-up. There are a number of possible drivers for such effects. For example, this could be a result of changes in the oxygen stoichiometry of the phases, as the oxygen reduction reaction process proceeds and the partial pressure of oxygen drops. Alternatively, this could be driven by the relative properties of the materials themselves and the rate-limiting processes under different conditions (e.g. oxygen exchange at low current density, electron transport at high current density).

Comparison of the EIS results (Fig. 4b, d and e) in the single cell testing approach demonstrated a general rule; the larger the impedance measured at OCV, the greater the activation loss shown on the polarisation curve (i.e. the greatest drop in voltage at low current density). As an example, the LNF64 and LNO4310 phases show the highest impedance values and also the most evident activation-type behaviour; LSCF6428 and LNO214 show the opposite trend. Although this correlation is largely expected, it is notable that the materials that perform best at this operating point (i.e. OCV) are also those with the most favourable oxygen transport behaviours. This remains the case even for LNO214 despite its relatively poor electrical conductivity in comparison with other cathode materials, as found by other studies in this area [15,18] and by comparison with other materials [42]. This indicates that the electron transport under this condition is not the rate-limiting step (understandable given the expected lower levels of electron transport under equilibrium conditions). It should also be noted, however, that whilst LNF64 shows poor performance at high voltages, the rate of decrease of current density with voltage reduces and, at lower voltages, the current density achieved exceeds that of LNO214. It is plausible that this alludes to the increased importance of electron transport at lower voltages, corresponding to high current densities. The pertinence of these observations will be further discussed later in this article.

4. Discussion

4.1. Comparison of symmetrical cell and single cell testing EIS results

In theory, and assuming all remaining factors are kept constant, the impedance response of an electrode in the symmetrical cell testing configuration should match that of its performance in the single cell testing configuration at the open circuit condition. In this work, commercial-grade substrates were employed for cathode characterisation to minimise the potential differences in performance that could be brought about by variations in the anode and electrolyte microstructures. Differences in performance in both cases should, primarily, be a result of the different cathode materials employed. Inspection of Fig. 4 shows a clear impact of the different cathode materials on the overall cell performance. A strong correlation between symmetrical cell and single cell testing EIS measurements was therefore expected. Indeed, this was shown to be broadly the case (Fig. 5). Those electrode materials that performed well in EIS symmetrical cell measurements generally also did so in the single cell testing conducted at OCV. Whilst it is important to

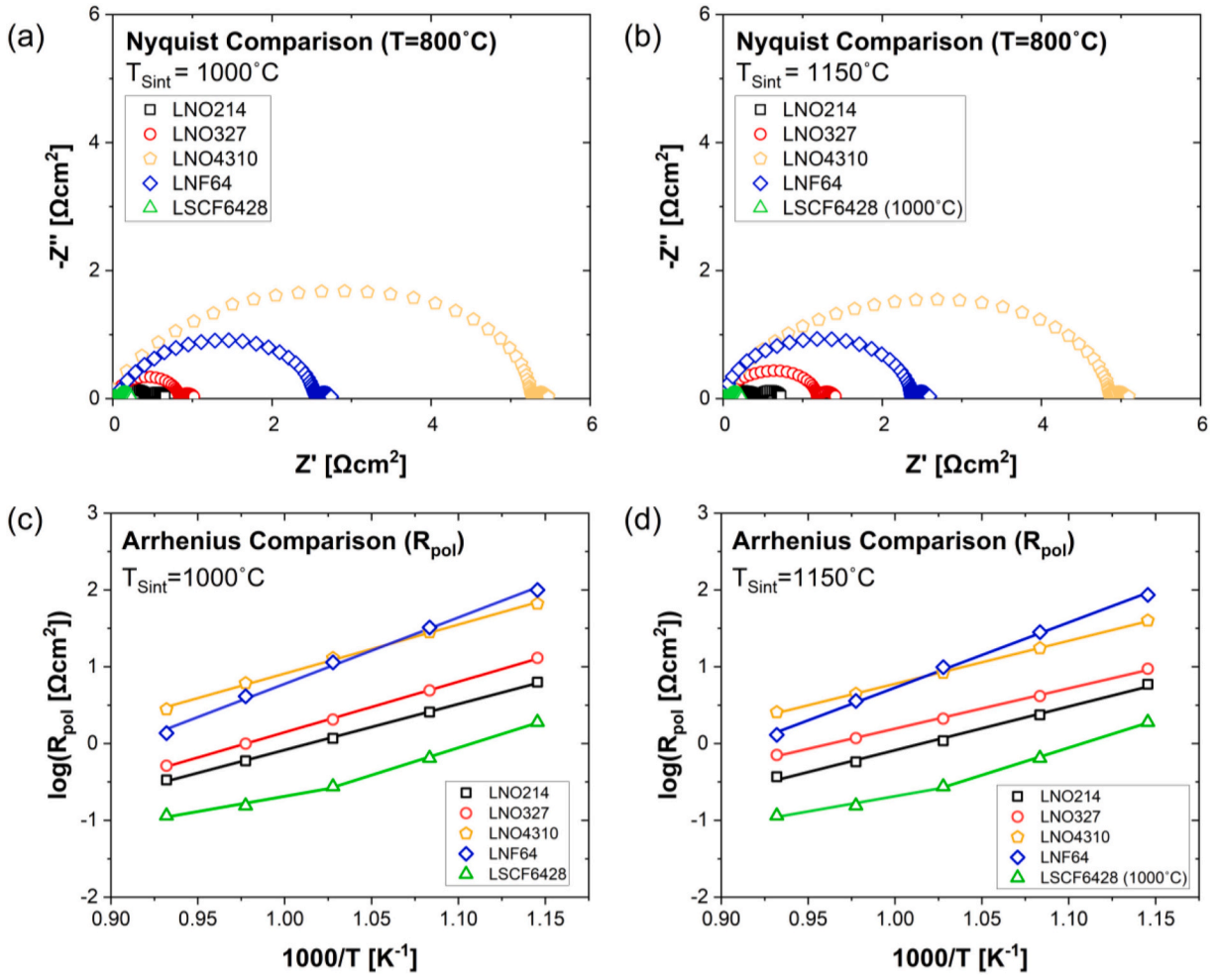

Fig. 3. Nyquist data recorded at an operated temperature of 800 °C taken from symmetrical cell tests of electrodes sintered at (a) 1000 °C and (b) 1150 °C, respectively. Arrhenius comparison of polarisation measurements from tests on electrodes sintered at (c) 1000 °C and (d) 1150 °C, respectively. NOTE: For the Nyquist plots of symmetrical cell tests, the ohmic contribution (R_o) of the impedance is removed for the convenience of comparison. A version of this figure has been published in a PhD thesis [35].

acknowledge some instances in which this relationship does not perfectly match this conclusion (e.g. compare LNF64–1150 with LNO4310–1000), the symmetrical cell tests were generally successful in identifying the single cell behaviour at the equilibrium point. This, therefore, appears to confirm the ability of symmetrical cell testing to overcome the issue of deconvolution and provides a justification for employing the approach to capture cell performance at OCV. However, it is noted that in this work, the cell performance is evidently dominated, or at least heavily influenced, by the cathode material studied. In other scenarios in which other components dominate cell performance (e.g. the anode), this relationship may be less evident. This instance may occur for more advanced cathode materials/microstructures or for lower performing substrates. Further comment on the significance of such a scenario is offered later.

4.2. Comparison of measurements at equilibrium and polarisation

Whilst it is evident that symmetrical cell testing broadly replicates measurements taken at OCV in single cell testing configuration, a question remains as to how well such equilibrium measurements reflect cell performance at greater polarisation. Fig. 6 demonstrates that measurements under different operating points are not always well correlated when comparing across different materials. Here, the current density measurements recorded in single cell testing (at two voltage points) are compared with the corresponding impedance measurements recorded at OCV in the same cell/test. Whilst EIS measurements recorded at OCV generally show a correlation with the current output at the higher voltage near the equilibrium operating point (i.e. Fig. 6a), the relationship is less well correlated at 0.7 V(i.e. Fig. 6b). Consideration of the aforementioned polarisation curve profiles offers some insight into this. Those materials that show very heavy activation losses at low current densities but more favourable performance in the linear region of the iV curve (e.g. $LaNi_{0.6}Fe_{0.4}O_3$ which shows a very curved polarisation profile), can show better current output at lower voltages. In fact, as was shown in Fig. 4e, LNF64 was observed to be the best performing lanthanum nickelate material, based on the achievable current density at 0.7 V (and below). Based on equilibrium measurements alone (symmetrical or single cell testing) this would not have been identified. The identification of promising electrodes based on such measurements alone has the potential of overlooking those materials and microstructures that perform well at low voltages which is the crucial operating point.

4.3. Significance with regard to assessing different cathode materials

The issues that have been outlined in Section 4.2 can be considered to be brought about due to the differing polarisation characteristics of the different electrodes studied. This can be summarised by a brief thought experiment in which three theoretical scenarios are considered (Fig. 7). In the first scenario (Fig. 7a), three cells are compared, with

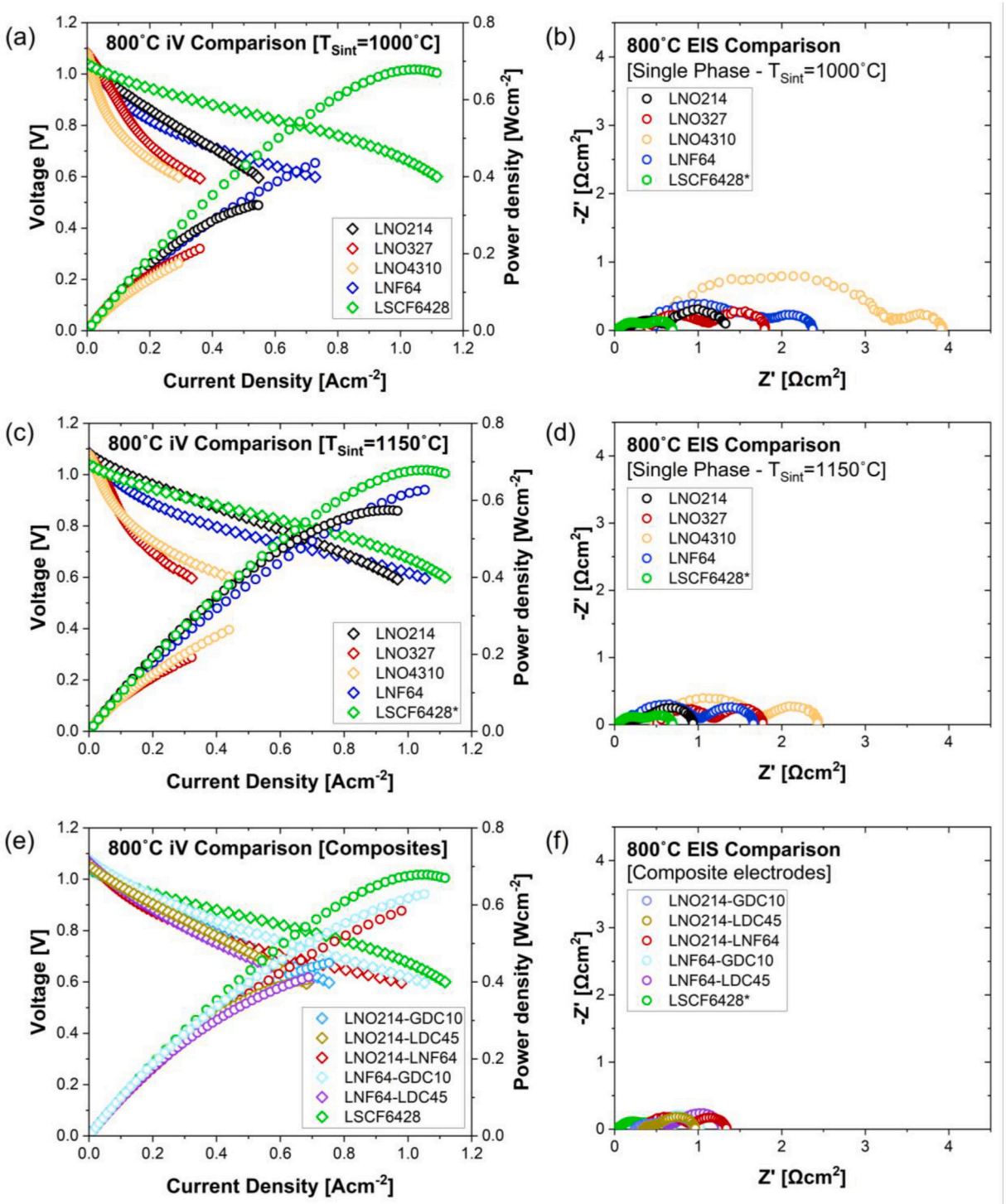

Fig. 4. Comparison of (a, c, e) polarisation curves and (b, d, f) EIS measurements (at OCV) recorded at an operating temperature of 800 °C for different electrodes. (*) In each instance the results are compared with an LSCF6428 electrode sintered at 1000 °C. In the case of the composite electrodes all electrodes were sintered at 1000 °C with the exception of those electrodes paired with LDC45 (T_{Sint} = 1150 °C). A version of this figure has been published in a PhD thesis [35].

each demonstrating perfectly linear iV characteristics. In the second (Fig. 7b), one of the cells studied ('Cell #1') does not display this same characteristic and has a more notable activation-type performance. The remaining two cells ('Cell #2' and 'Cell #3' display the more conventional linear behaviour). A third scenario is also possible in which concentration losses cause the opposite effect, leading to a sudden voltage decrease towards zero with increasing current (Fig. 7c). In any of these scenarios, an SOFC researcher may attempt to find the best-performing cell to continue with their optimisation activities; however, if only symmetrical cell testing is employed, the researcher risks overlooking the polarisation results shown in Fig. 7. To conduct the thought experiment, several assumptions are made. Firstly, symmetrical cell testing is assumed to effectively re-create the single cell test result at equilibrium (as was shown to be broadly true in Section 4.1). Secondly, given the impedance response represents the gradient at a point along the polarisation curve (i.e. the greater the gradient, the greater the EIS

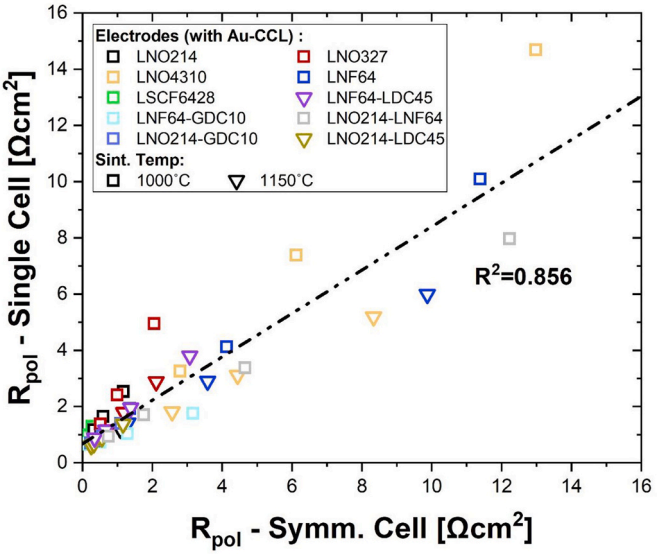

Fig. 5. Comparison of performance of electrodes sintered at 1000 °C and 1150 °C in the symmetrical cell and single cell testing configuration. A version of this figure has been published in a PhD thesis [35].

response), this will be proposed as a proxy for EIS in these scenarios.

In the first scenario, current density measurements at any point along the polarisation curve lead to the same conclusion; Cell #1 is superior by any measurement approach in this scenario. Thus, if the researcher in Scenario #1 considered only R_{pol} values from the symmetrical cell testing approach, the outcome would have been the same as had they additionally taken current density/impedance measurements under polarisation. The conclusion in this instance is independent of the current drawn. If, on the other hand, the researcher had employed the same method in the second scenario where (unbeknownst to them) 'Cell #1' displayed high activation losses but lower losses at higher current density, a more ambiguous outcome may have resulted. In that instance, the researcher's results identifying Cell #2 as the optimal choice based on symmetrical cell testing alone would have neglected the opportunity to select and optimise a cell that performed better under greater polarisation. This observation could not have been attained by conducting symmetrical cell testing alone. Likewise, Scenario #3 could also offer further complications when comparing results at a single operating point. The critical point is that symmetrical cell testing alone does not enable a full understanding of which of these scenarios occurs, particularly if comparing dissimilar materials.

4.4. The benefits of symmetrical cell testing

Whilst it is evident that there are some limitations of EIS measurements at OCV, it is important to note that the state-of-the-art material (i.e. $La_{0.6}Sr_{0.4}Co_{0.2}Fe_{0.8}O_{3-\delta}$) offered the best performance in both testing approaches. Importantly, materials that offer promise in replacing the state-of-the-art LSCF6428 phase will likely show excellent behaviour at both OCV (i.e. low R_{pol} values) and under polarisation. Therefore, symmetrical cell testing can be considered as a simple and useful screening technique. Further, and as was discussed in Section 4.4, it can be suggested that, in some circumstances, the symmetrical cell testing can be used to identify routes to improving electrode performance. It is notable that, in the present study, a wide range of materials with very different behaviour has been employed. In studies with a more limited body of materials or electrode configurations (e.g. small changes in composition or microstructure), the symmetrical cell testing approach is likely to be of more reliable significance. This is exemplified in the present study (and our prior work [33]) in that improvements in performance achieved by increasing sintering temperature were captured

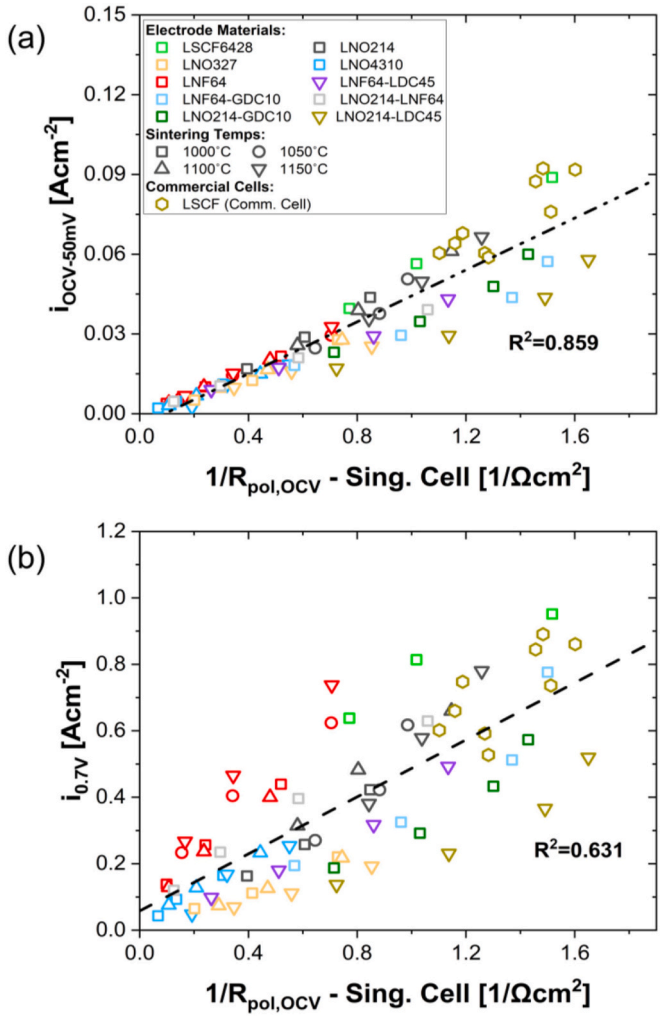

Fig. 6. Comparison of single cell testing measurements (EIS measurements vs current density); (a) $i_{OCV\text{-}50mV}$ and (b) $i_{0.7V}$. The displayed measurements cover three operating temperatures (700, 750, 800 °C), five different materials ($La_2NiO_{4+\delta}$, $La_3Ni_2O_{7-\delta}$, $La_4Ni_3O_{10-\delta}$, $LaNi_{0.6}Fe_{0.4}O_{3-\delta}$, $La_{06}Sr_{0.4}Co_{0.2}Fe_{0.8}O_{3-\delta}$), composite electrodes ($La_2NiO_{4+\delta}$-$Gd_{0.1}Ce_{0.9}O_2$, $La_2NiO_{4+\delta}$-$La_{0.45}Ce_{0.55}O_{2-\delta}$, $La_2NiO_{4+\delta}$-$LaNi_{0.6}Fe_{0.4}O_{3-\delta}$, $LaNi_{0.6}Fe_{0.4}O_{3-\delta}$-$Gd_{0.1}Ce_{0.9}O_{2-\delta}$, $LaNi_{0.6}Fe_{0.4}O_{3-\delta}$-$La_{0.45}Ce_{0.55}O_{2-\delta}$) and four different sintering temperatures (1000, 1050, 1100, 1150 °C). For a full list of the tests employed, see the Supplementary Materials. A version of this figure has been published in a PhD thesis [35].

by both symmetrical and single cell testing approaches. This can be further appreciated in Supplementary Fig. S17 where the individual materials are singled out from Fig. 6b. To re-iterate the challenges identified, however, comparing dissimilar phases in this way could lead to the aforementioned issues if studying R_{pol} values in isolation. A further point to note is in relation to the relative performance of the anode in single cell testing. If, unlike in this study, the cathode polarisation resistance is far below that of the anode contribution, the performance of the single cell may be dominated (or limited) by the anode and, in such a case, the employment of single cell testing alone may be unlikely to identify the impact of the cathode. In such an instance, symmetrical cell testing may provide clearer value.

More advanced utilisation of symmetrical cell testing results is also a possibility that has been explored in the literature. It has to be noted that it has been shown to be feasible to identify activation and diffusion losses by detailed EIS analysis and modelling [43–46]. This involved EIS measurements under a variety of operating parameters thus simulating different scenarios at OCV which represent scenarios with large diffusion losses (for example, dilution of oxygen for cathode) and large

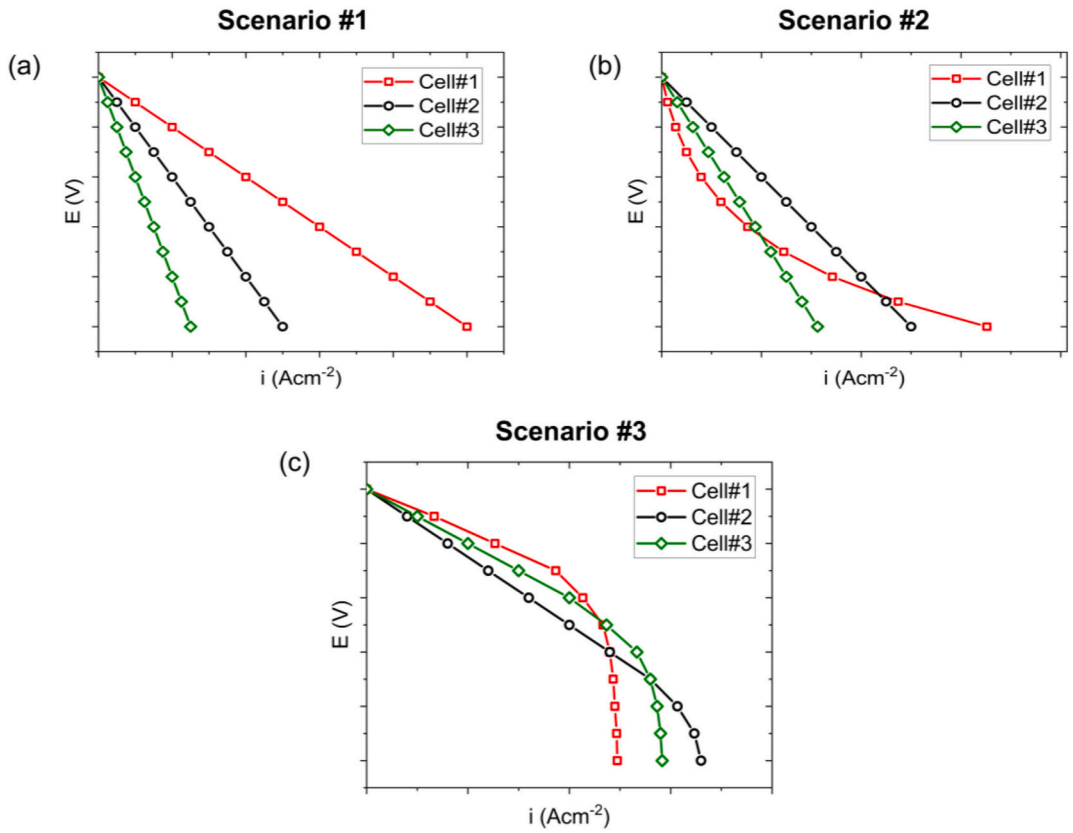

Fig. 7. Three plausible scenarios when comparing the performance of cell/electrode performance; (a) Scenario #1 demonstrates a case where three cells are compared with consistent linear polarisation behaviour, (b) Scenario #2 demonstrates a situation where one of the compared cells has a strong activation behaviour and (c) Scenario #3 provides a case where concentration losses are evident at different voltage conditions.

activation losses (for example, low temperatures). It has also been shown that most parameters that govern the performance of SOFC can be deduced under OCV conditions. In fact, Leonide et al. [47–49] have shown that the performance of an SOFC/SOEC can be modelled by parameters gained from EIS measurements at OCV – apart from the symmetry factor for the applied Butler-Vollmer approach, which had to be determined under polarisation.

Finally, despite some shortfalls described in this article, the simplified practicalities of performing symmetrical cell testing especially for screening cathode materials, in comparison with single cell tests, should not be overlooked. The approach helps to avoid the use of hydrogen, the reduction steps for NiO anodes, and the sealing requirements of the anode and cathode compartment, which can introduce numerous complications in terms of both safety and obtaining good quality data. Whilst the use of symmetrical cell testing should be treated with some caution (in particular, basic comparisons of R_{pol} values across different types of materials), there remain some evident benefits.

5. Conclusion

In this paper the role of symmetrical cell testing in identifying improved SOFC electrode materials has been explored. Whilst it is often noted in the wider literature that the shortfall of symmetrical cell testing lies in its limited relevance to performance of electrodes under polarisation, here we provide critical analysis on how suitable this methodology truly is in isolating the best electrode materials. The analysis provided in this study shows that, whilst consideration of R_{pol} values in symmetrical cell testing can identify certain relationships that may be of interest in electrode development (e.g. the improvement of performance that can be achieved via increased sintering temperature), this approach does not *always* successfully reveal those materials that show the best performance under polarisation. This was shown via an assessment of the performance of dissimilar materials.

Whilst a cautious approach must be taken when considering symmetrical cell testing, it can be noted that in this study the state-of-the-art material $La_{0.6}Sr_{0.4}Co_{0.2}Fe_{0.8}O_{3-\delta}$ was the best-performing in both the symmetrical and single cell testing approaches. It is likely that true 'promising materials' that can serve as a replacement for the state-of-the-art will show low polarisation resistance under equilibrium conditions and will also show high current output away from the equilibrium-state. Nevertheless, some care should be taken in treating symmetrical cell test results as a 'silver bullet' to predicting electrode performance. More advanced experimental set-ups and utilisation of other results is encouraged.

Finally, two areas of further research opportunity are noted in relation to this study. Firstly, it is acknowledged that this research was conducted with 16 cm^2 electrodes; it may be of further interest to consider if similar observations occur when employing electrodes and cells of smaller size. Additionally, it is of further significance to consider if the observations in this article are transferrable to the case where electrode performance is further improved (e.g. $R_{pol} < 0.1\Omega cm^2$) or, alternatively, if the relationships identified are obscured.

Funding

This work was supported by the EPSRC via both the Centre for Doctoral Training on Fuel Cells and their Fuels, grant reference EP/L015749/1, and the JUICED Hub Grant, ref. EP/R023662/1. Additionally, Dr. Sarruf acknowledges the funding received from the European Union's Horizon 2020 research and innovation programme under the Marie Skłodowska-Curie grant agreement No 101032423.

CRediT authorship contribution statement

C.M. Harrison: Writing – review & editing, Writing – original draft, Visualization, Investigation, Formal analysis, Data curation, Conceptualization. **D. Klotz:** Writing – review & editing. **B.J.M. Sarruf:** Writing – review & editing. **P.R. Slater:** Writing – review & editing, Supervision. **R. Steinberger-Wilckens:** Writing – review & editing, Supervision, Funding acquisition.

Declaration of competing interest

The authors declare that they have no known competing financial interests or personal relationships that could have appeared to influence the work reported in this paper.

Data availability

The raw data employed in this study is available as an e-component of this article.

Appendix A. Supplementary data

Supplementary data to this article can be found online at https://doi.org/10.1016/j.ssi.2024.116551.

References

[1] J. Weissbart, R. Ruka, A solid electrolyte fuel cell, J. Electrochem. Soc. 109 (1962) 723–726, https://doi.org/10.1149/1.2425537.

[2] L. Blum, L.G.J. De Haart, J. Malzbender, N.H. Menzler, J. Remmel, R. Steinberger-Wilckens, Recent results in Jülich solid oxide fuel cell technology development, J. Power Sources 241 (2013) 477–485, https://doi.org/10.1016/j.jpowsour.2013.04.110.

[3] F. Kunz, R. Peters, D. Schäfer, S. Zhang, N. Kruse, L.G.J. de Haart, V. Vibhu, R.-A. Eichel, N.H. Menzler, C. Lenser, D. Naumenko, T. Kadyk, N. Margaritis, S. Gross-Barsnick, Progress in research and development of solid oxide cells, stacks and systems at Forschungszentrum Jülich, ECS Trans. 111 (2023) 1667–1676, https://doi.org/10.1149/11106.1667ecst.

[4] A. Ndubuisi, S. Abouali, K. Singh, V. Thangadurai, Recent advances, practical challenges, and perspectives of intermediate temperature solid oxide fuel cell cathodes, J. Mater. Chem. A Mater. 10 (2022) 2196–2227, https://doi.org/10.1039/d1ta08475e.

[5] S.B. Adler, Reference electrode placement in thin solid electrolytes, J. Electrochem. Soc. 149 (2002) E166–E172, https://doi.org/10.1149/1.1467368.

[6] S. Adler, Reference electrode placement and seals in electrochemical oxygen generators, Solid State Ionics 134 (2000) 35–42, https://doi.org/10.1016/S0167-2738(00)00711-6.

[7] J. Winkler, P.V. Hendriksen, N. Bonanos, M. Mogensen, Geometric requirements of solid electrolyte cells with a reference electrode, J. Electrochem. Soc. 145 (1998) 1184–1192, https://doi.org/10.1149/1.1838436.

[8] M. Nagata, Y. Itoh, H. Iwahara, Dependence of observed overvoltages on the positioning of the reference electrode on the solid electrolyte, Solid State Ionics 67 (1994) 215–224, https://doi.org/10.1016/0167-2738(94)90008-6.

[9] S.P. Jiang, Placement of reference electrode, electrolyte thickness and three-electrode cell configuration in solid oxide fuel cells: a brief review and update on experimental approach, J. Electrochem. Soc. 164 (2017) F834–F844, https://doi.org/10.1149/2.1331707jes.

[10] A. Hauch, M. Mogensen, Testing of electrodes, cells, and short stacks, in: Advances in Medium and High Temperature Solid Oxide Fuel Cell Technology, 2016, pp. 31–76, https://doi.org/10.1007/978-3-319-46146-5_2 (accessed December 18, 2023).

[11] D. Klotz, A. Weber, E. Ivers-Tiffée, Practical guidelines for reliable electrochemical characterization of solid oxide fuel cells, Electrochim. Acta 227 (2017) 110–126, https://doi.org/10.1016/j.electacta.2016.12.148.

[12] X. Xu, Y. Pan, Y. Zhong, R. Ran, Z. Shao, Ruddlesden-popper perovskites in electrocatalysis, Mater. Horiz. 7 (2020) 2519–2565, https://doi.org/10.1039/d0mh00477d.

[13] D.O. Bannikov, V.A. Cherepanov, Thermodynamic properties of complex oxides in the La-Ni-O system, J. Solid State Chem. 179 (2006) 2721–2727, https://doi.org/10.1016/j.jssc.2006.05.026.

[14] S. Skinner, Oxygen diffusion and surface exchange in La2−xSrxNiO4+δ, Solid State Ionics 135 (2000) 709–712, https://doi.org/10.1016/S0167-2738(00)00388-X.

[15] S. Takahashi, S. Nishimoto, M. Matsuda, M. Miyake, Electrode properties of the ruddlesden-popper series, Lan+1NinO3n+1 (n=1, 2, and 3), as intermediate-temperature solid oxide fuel cells, J. Am. Ceram. Soc. 93 (2010) 2329–2333, https://doi.org/10.1111/j.1551-2916.2010.03743.x.

[16] J. Song, D. Ning, B. Boukamp, J.M. Bassat, H.J.M. Bouwmeester, Structure, electrical conductivity and oxygen transport properties of Ruddlesden-popper phases ln n+1 Ni n O3 n +1(ln = La, Pr and Nd; N = 1, 2 and 3), J. Mater. Chem. A Mater. 8 (2020) 22206–22221, https://doi.org/10.1039/d0ta06731h.

[17] H. Zhao, F. Mauvy, C. Lalanne, J.M. Bassat, S. Fourcade, J.C. Grenier, New cathode materials for ITSOFC: phase stability, oxygen exchange and cathode properties of La2 - xNiO4 + δ, Solid State Ionics 179 (2008) 2000–2005, https://doi.org/10.1016/j.ssi.2008.06.019.

[18] G. Amow, I.J. Davidson, S.J. Skinner, A comparative study of the Ruddlesden-popper series, Lan+1NinO3n+1 (n = 1, 2 and 3), for solid-oxide fuel-cell cathode applications, Solid State Ionics 177 (2006) 1205–1210, https://doi.org/10.1016/j.ssi.2006.05.005.

[19] E.N. Armstrong, K.L. Duncan, E.D. Wachsman, Effect of a and B-site cations on surface exchange coefficient for ABO 3 perovskite materials, Phys. Chem. Chem. Phys. 15 (2013) 2298–2308, https://doi.org/10.1039/c2cp42919e.

[20] L. Tai, M.M. Nasrallah, H.U. Anderson, D.M. Sparlin, S.R. Sehlin, Structure and electrical properties of La1 − xSrxCo1 − yFeyO3. Part 2. The system La1 − xSrxCo0.2Fe0.8O3, Solid State Ionics 76 (1995) 273–283, https://doi.org/10.1016/0167-2738(94)00245-N.

[21] C.M. Harrison, P.R. Slater, R. Steinberger-Wilckens, Lanthanum nickelates and their application in solid oxide cells – the LaNi1-xFexO3 system and other ABO3-type nickelates, Solid State Ionics 373 (2021), https://doi.org/10.1016/j.ssi.2021.115799.

[22] S. Molin, P.Z. Jasinski, Improved performance of LaNi0.6Fe0.4O3 solid oxide fuel cell cathode by application of a thin interface cathode functional layer, Mater. Lett. 189 (2017) 252–255, https://doi.org/10.1016/j.matlet.2016.11.101.

[23] X. Zhang, L. Zhang, J. Meng, W. Zhang, F. Meng, X. Liu, J. Meng, Highly enhanced electrochemical property by mg-doping La2Ni1-xMgxO4+Δ (x = 0.0, 0.02, 0.05 and 0.10) cathodes for intermediate-temperature solid oxide fuel cells, Int. J. Hydrog. Energy 42 (2017) 29498–29510, https://doi.org/10.1016/j.ijhydene.2017.10.091.

[24] Z. Lou, J. Peng, N. Dai, J. Qiao, Y. Yan, Z. Wang, J. Wang, K. Sun, High performance La 3Ni 2O 7 cathode prepared by a facile sol-gel method for intermediate temperature solid oxide fuel cells, Electrochem. Commun. 22 (2012) 97–100, https://doi.org/10.1016/j.elecom.2012.06.004.

[25] R.K. Sharma, M. Burriel, L. Dessemond, J.M. Bassat, E. Djurado, Lan+1NinO3n+1 (n = 2 and 3) phases and composites for solid oxide fuel cell cathodes: facile synthesis and electrochemical properties, J. Power Sources 325 (2016) 337–345, https://doi.org/10.1016/j.jpowsour.2016.06.047.

[26] X. Lou, S. Wang, Z. Liu, L. Yang, M. Liu, Improving La0.6Sr0.4Co0.2Fe0.8O3 - δ cathode performance by infiltration of a Sm0.5Sr0.5CoO3 - δ coating, Solid State Ionics 180 (2009) 1285–1289, https://doi.org/10.1016/j.ssi.2009.06.014.

[27] A. Chrzan, J. Karczewski, M. Gazda, D. Szymczewska, P. Jasinski, Investigation of thin perovskite layers between cathode and doped ceria used as buffer layer in solid oxide fuel cells, J. Solid State Electrochem. 19 (2015) 1807–1815, https://doi.org/10.1007/s10008-015-2815-x.

[28] R.K. Sharma, M. Burriel, E. Djurado, La4Ni3O10-δ as an efficient solid oxide fuel cell cathode: electrochemical properties versus microstructure, J. Mater. Chem. A Mater. 3 (2015) 23833–23843, https://doi.org/10.1039/c5ta07862h.

[29] A. Mater, A.H. Othmani, A. Boukhachem, A. Madani, Cathode performance study of La0.6Sr0.4Co0.8Fe0.2O3-δ with various electrolyte-doped ceria Ce0.8Sm0.17Ln0.03O1.9 for IT-solid oxide fuel cell, J. Electron. Mater. 49 (2020) 4123–4133, https://doi.org/10.1007/s11664-020-08167-x.

[30] M.P. Pechini, Method of preparing lead and alkaline earth titanates and niobates and coating method using the same to form a capacitor, United States Patent Office, 3,330,697, 1967, https://patents.google.com/patent/US3330697A/en (accessed March 10, 2024).

[31] E. Pikalova, N. Bogdanovich, A. Kolchugin, L. Ermakova, A. Khrustov, A. Farlenkov, D. Bronin, Methods to increase electrochemical activity of lanthanum nickelate-ferrite electrodes for intermediate and low temperature SOFCs, Int. J. Hydrog. Energy 46 (2021) 35923–35937, https://doi.org/10.1016/j.ijhydene.2021.01.226.

[32] V. Vibhu, A. Flura, A. Rougier, C. Nicollet, S. Fourcade, T. Hungria, J.C. Grenier, J. M. Bassat, Electrochemical ageing study of mixed lanthanum/praseodymium nickelates La2-xPrxNiO4+δ as oxygen electrodes for solid oxide fuel or electrolysis cells, J. Energy Chem. 46 (2020) 62–70, https://doi.org/10.1016/j.jechem.2019.10.012.

[33] C.M. Harrison, B.J.M. Sarruf, D. Klotz, P.R. Slater, R. Steinberger-Wilckens, The effects of sintering temperature and current contacting layer on the performance of lanthanum nickelate electrodes in solid oxide fuel cells, Solid State Ionics 403 (2023), https://doi.org/10.1016/j.ssi.2023.116386.

[34] M. Schönleber, D. Klotz, E. Ivers-Tiffée, A method for improving the robustness of linear Kramers-Kronig validity tests, Electrochim. Acta 131 (2014) 20–27.

[35] C.M. Harrison, A Study of Lanthanum Nickelate Cathodes for Employment in Solid Oxide Fuel Cells [doctoral thesis, in press], University of Birmingham, 2023.

[36] R.K. Sharma, M. Burriel, L. Dessemond, J.M. Bassat, E. Djurado, Lan+1NinO3n+1 (n = 2 and 3) phases and composites for solid oxide fuel cell cathodes: facile synthesis and electrochemical properties, J. Power Sources 325 (2016) 337–345, https://doi.org/10.1016/j.jpowsour.2016.06.047.

[37] A. Aguadero, J.A. Alonso, M.J. Escudero, L. Daza, Evaluation of the La2Ni1 - xCuxO4 + δ system as SOFC cathode material with 8YSZ and LSGM as electrolytes, Solid State Ionics 179 (2008) 393–400, https://doi.org/10.1016/j.ssi.2008.01.099.

[38] Y. Chen, Y. Bu, Y. Zhang, R. Yan, D. Ding, B. Zhao, S. Yoo, D. Dang, R. Hu, C. Yang, M. Liu, A highly efficient and robust nanofiber cathode for solid oxide fuel cells, Adv. Energy Mater. 7 (2017), https://doi.org/10.1002/aenm.201601890.

[39] H. Orui, K. Watanabe, R. Chiba, M. Arakawa, Application of LaNi(Fe)O3 as SOFC cathode, J. Electrochem. Soc. 151 (2004) A1412–A1417, https://doi.org/10.1149/1.1779628.

[40] Y. Li, J.W. Cai, J.A. Alonso, H.Q. Lian, X.G. Cui, J.B. Goodenough, Evaluation of LaNi0.6M0.4O3 (M = Fe, co) cathodes in LSGM-electrolyte-supported solid-oxide fuel cells, Int. J. Hydrog. Energy 42 (2017) 27334–27342, https://doi.org/10.1016/j.ijhydene.2017.09.031.

[41] S.P. Simner, J.F. Bonnett, N.L. Canfield, K.D. Meinhardt, V.L. Sprenkle, J. W. Stevenson, Optimized lanthanum ferrite-based cathodes for anode-supported SOFCs, Electrochem. Solid-State Lett. 5 (2002) A173–A175, https://doi.org/10.1149/1.1483156.

[42] C.M. Harrison, P.R. Slater, R. Steinberger-Wilckens, A review of solid oxide fuel cell cathode materials with respect to their resistance to the effects of chromium poisoning, Solid State Ionics 354 (2020), https://doi.org/10.1016/j.ssi.2020.115410.

[43] A. Leonide, V. Sonn, A. Weber, E. Ivers-Tiffée, Evaluation and modeling of the cell resistance in anode-supported solid oxide fuel cells, J. Electrochem. Soc. 155 (2008) B36–B41, https://doi.org/10.1149/1.2801372.

[44] V. Sonn, A. Leonide, E. Ivers-Tiffée, Combined deconvolution and CNLS fitting approach applied on the impedance response of technical Ni/8YSZ cermet electrodes, J. Electrochem. Soc. 155 (2008) B675–B679, https://doi.org/10.1149/1.2908860.

[45] C. Grosselindemann, N. Russner, S. Dierickx, F. Wankmüller, A. Weber, Deconvolution of gas diffusion polarization in Ni/gadolinium-doped ceria fuel electrodes, J. Electrochem. Soc. 168 (2021) 124506, https://doi.org/10.1149/1945-7111/ac3d02.

[46] S. Golani, F. Wankmüller, W. Herzhof, C. Dellen, N.H. Menzler, A. Weber, Impact of GDC interlayer microstructure on strontium Zirconate interphase formation and cell performance, J. Electrochem. Soc. 170 (2023) 104501, https://doi.org/10.1149/1945-7111/acfc2c.

[47] A. Leonide, Y. Apel, E. Ivers-Tiffee, SOFC modeling and parameter identification by means of impedance spectroscopy, ECS Trans. 19 (2009) 81–109, https://doi.org/10.1149/1.3247567.

[48] A. Leonide, SOFC Modelling and Parameter Identification by Means of Impedance Spectroscopy [Doctoral Thesis], Karlsruher Institut für Technologie (KIT), 2010. https://publikationen.bibliothek.kit.edu/1000019173 (accessed March 10, 2024).

[49] J.-C. Njodzefon, D. Klotz, A. Kromp, A. Weber, E. Ivers-Tiffée, Electrochemical modeling of the current-voltage characteristics of an SOFC in fuel cell and electrolyzer operation modes, J. Electrochem. Soc. 160 (2013) F313–F323, https://doi.org/10.1149/2.018304jes.